Since January 2020 Elsevier has created a COVID-19 resource centre with free information in English and Mandarin on the novel coronavirus COVID-19. The COVID-19 resource centre is hosted on Elsevier Connect, the company's public news and information website.

Virus Research 177 (2013) 127–137

Contents lists available at ScienceDirect

Virus Research

journal homepage: www.elsevier.com/locate/virusres

Contributions of the S2 spike ectodomain to attachment and host range of infectious bronchitis virus

N. Promkuntod, I.N. Ambepitiya Wickramasinghe, G. de Vrieze, A. Gröne, M.H. Verheije*

Pathology Division, Department of Pathobiology, Faculty of Veterinary Medicine, Utrecht University, Yalelaan 1, 3584 CL Utrecht, The Netherlands

ARTICLE INFO

Article history:
Received 23 July 2013
Received in revised form 3 September 2013
Accepted 4 September 2013
Available online 13 September 2013

Keywords:
Infectious bronchitis virus
Avian coronavirus
Beaudette
M41
Spike
Attachment

ABSTRACT

The spike protein is the major viral attachment protein of the avian coronavirus infectious bronchitis virus (IBV) and ultimately determines viral tropism. The S1 subunit of the spike is assumed to be required for virus attachment. However, we have previously shown that this domain of the embryo- and cell culture adapted Beaudette strain, in contrast to that of the virulent M41 strain, is not sufficient for binding to chicken trachea (Wickramasinghe et al., 2011). In the present study, we demonstrated that the lack of binding of Beaudette S1 was not due to absence of virus receptors on this tissue nor due to the production of S1 from mammalian cells, as S1 proteins expressed from chicken cells also lacked the ability to bind IBV-susceptible embryonic tissue. Subsequently, we addressed the contribution of the S2 subunit of the spike in IBV attachment. Recombinant IBV Beaudette spike ectodomains, comprising the entire S1 domain and the S2 ectodomain, were expressed and analyzed for binding to susceptible embryonic chorio-allantoic membrane (CAM) in our previously developed spike histochemistry assay. We observed that extension of the S1 domain with the S2 subunit of the Beaudette spike was sufficient to gain binding to CAM. A previously suggested heparin sulfate binding site in Beaudette S2 was not required for the observed binding to CAM, while sialic acids on the host tissues were essential for the attachment. To further elucidate the role of S2 the spike ectodomains of virulent IBV M41 and chimeras of M41 and Beaudette were analyzed for their binding to CAM, chicken trachea and mammalian cell lines. While the M41 spike ectodomain showed increased attachment to both CAM and chicken trachea, no binding to mammalian cells was observed. In contrast, Beaudette spike ectodomain had relatively weak ability to bind to chicken trachea, but displayed marked extended host range to mammalian cells. Binding patterns of chimeric spike ectodomains to these tissues and cells indicate that S2 subunits most likely do not contain an additional independent receptor-binding site. Rather, the interplay between S1 and S2 subunits of spikes from the same viral origin might finally determine the avidity and specificity of virus attachment and thus viral host range.

1. Introduction

The avian coronavirus infectious bronchitis virus (IBV) is an important viral pathogen for the poultry industry worldwide (Jackwood, 2012). IBV is an enveloped, positive strand RNA virus belonging to the genus *Gammacoronavirus*, family *Coronaviridae*, order *Nidovirales* (Adams and Carstens, 2012). The prototype IBV strain Massachusetts 41 (M41) causes a highly contagious respiratory infection in chickens, while the pathology of other IBV strains ranges from mild respiratory symptoms to diseases affecting mainly oviduct and kidney, sometimes resulting in the death of the animal (reviewed in Sjaak de Wit et al., 2011).

Coronaviruses have a strict species tropism, which is largely determined by the interaction of the viral attachment protein spike (S) with the host cell (recently reviewed in Belouzard et al., 2012; Graham and Baric, 2010). The coronaviral S protein is a highly glycosylated class I viral fusion protein (Bosch et al., 2003), which in some coronaviruses, including IBV, is cleaved during synthesis into an S1 and an S2 subunit by the host serine protease furin (de Haan et al., 2004; Yamada and Liu, 2009). The S1 is essential for initial attachment of the virus, while the membrane anchored S2 subunit or domain, containing the remaining part of the ectodomain, a transmembrane domain and an endodomain, drives virus-cell fusion (reviewed in Heald-Sargent and Gallagher, 2012). All coronaviral receptor-binding domains (RBD) currently identified are located within the S1 subunit or domain (reviewed in Belouzard et al., 2012; Graham and Baric, 2010). For IBV, the exact location of the RBD has, however, not yet been elucidated. Heterogeneity between IBV strains is mainly associated with differences in S1, but IBV spike

* Corresponding author. Tel.: +31 30 253 4296; fax: +31 30 253 2333.
E-mail address: m.h.verheije@uu.nl (M.H. Verheije).

0168-1702/$ – see front matter © 2013 Elsevier B.V. All rights reserved.
http://dx.doi.org/10.1016/j.virusres.2013.09.006

cleavage (into an approximately 520 amino acid (aa) S1 and an approximately 620 aa S2 subunit Cavanagh et al., 1986) appears to be independent of geographical origin, serotype or the pathogenic profile (Jackwood et al., 2001). Ultimately, the host and tissue range of coronaviruses is determined by the expression of specific receptors. Specific protein receptors have been identified for many alpha- and betacoronaviruses (Belouzard et al., 2012; Graham and Baric, 2010 and references therein). For avian gammacoronaviruses, no such protein receptor has been elucidated, but alpha-2,3 linked sialic acids have been shown to be essential for attachment and subsequent infection of avian cells (Abd El Rahman et al., 2009; Wickramasinghe et al., 2011; Winter et al., 2006, 2008). In addition, it was recently demonstrated that expression of human DC-SIGN-like lectins renders cells susceptible to IBV infection (Zhang et al., 2012), but no avian counterpart of this molecule has yet been identified. Thus, the molecular determinants for the host and tissue range of IBV are yet far from understood.

Most clinical IBV strains can only be replicated in embryonated eggs or primary chicken embryonic kidney cells upon adaptation to these systems (Cook et al., 1976; Kawamura et al., 1961; Sawaguchi et al., 1985). The best studied avian coronavirus strain, IBV Beaudette, however, has the ability to infect cultured cell lines, including the mammalian cell lines Vero and BHK-21 (Fang et al., 2005; Otsuki et al., 1979). Beaudette was derived from the Massachusetts strain M41 by serial passage in embryonated eggs for at least 150 times (Beaudette and Hudson, 1937), rendering the virus highly pathogenic for chicken embryos, but avirulent for chickens (Geilhausen et al., 1973). M41 and Beaudette have 96% amino acid identity in their spikes, with 25 aa differences in S1 (excluding the signal sequence) and 18 aa changes in S2. The essential role of the spike in determining the extended host range of IBV Beaudette was shown upon exchange of spike genes in the recombinant Beaudette viral genome. Substitution of the spike protein of M41 (Casais et al., 2003; Hodgson et al., 2004) or 4/91 (Armesto et al., 2011) into the Beaudette genome abolished the ability of Beaudette to infect mammalian cell lines, but did not confer pathogenicity in chickens (Armesto et al., 2011; Hodgson et al., 2004).

Previously, we showed that the S1 protein of the embryo- and cell culture-adapted Beaudette, in contrast to that of the virulent M41, is not able to bind to chicken respiratory tract tissues (Wickramasinghe et al., 2011). While the observed difference was in line with the reported changes in the ability of these two virus strains to infect and replicate in chickens, the results were to some extent unexpected. IBV Beaudette can be propagated in trachea organ cultures (TOCs; Cook et al., 1976) and embryonated eggs (reviewed in Guy, 2008), and has extended tropism for mammalian cells (Cunningham et al., 1972; Otsuki et al., 1979), but its requirements for attachment and subsequent entry are still under debate. While heparan sulfate (HS) binding was proposed to be required for its extended tropism (Madu et al., 2007), studies with recombinant Beaudette indicate that the proposed HS binding site in S2 is not crucial for entry of the virus (Yamada and Liu, 2009). Here, we aimed at further elucidating the requirements for IBV Beaudette spike attachment using our recently developed spike histochemistry assay (Wickramasinghe et al., 2011). Particular focus was on the contribution of the S2 part of the ectodomain of the spike. Our results show that the complete ectodomain was required to confer binding of the Beaudette spike to chicken tissues. Host sialic acids, but not HS, were required for the attachment. Analysis of the spike ectodomain of M41 and chimeric spikes suggests that the IBV S2 ectodomain does not contain an additional independent binding site, but rather increases the avidity of S1. Interestingly, ectodomains comprised of only Beaudette spike sequences had the ability to bind to mammalian cell cultures, suggesting that both S1 and S2 contain determinants important for the extended host range of Beaudette.

2. Materials and Methods

2.1. Cells and cell culture pellets

Human Embryonic Kidney (HEK) 293T cells, Vero-CCL81 and BHK21 were maintained in Dulbecco's Modified Eagle Medium (DMEM) (BioWhittaker) supplemented with 2% glutamine, 10% Fetal Calf Serum (FCS) (BioWhittaker) and 0.1 mg/ml gentamicin (Gibco Invitrogen). Chicken fibroblast DF1 cells were cultured in DMEM supplemented with 2% glutamine, 0.1 mg/ml gentamicin, 10% FCS and 1% sodium pyruvate (Sigma–Aldrich). To obtain cell pellets for spike histochemistry, cells from monolayers of Vero-CCL81 and BHK21 were collected by scraping and subsequent centrifugation at 200 × *g*. Pellets were fixed in formalin for 24 h and embedded in paraffin.

2.2. Virus stocks and inoculation of embryonated chicken eggs

The allantoic cavity of 11-day-old SPF embryonated chicken eggs (ECE) were inoculated with 200 EID_{50} of the IBV strains M41 and Beaudette (Animal Health Service, Deventer, The Netherlands). Inoculated ECE were candled twice daily and at 48 h post-inoculation chorio-allantoic membranes (CAM) were fixed in formalin for 24 h prior to paraffin-embedding of the tissue.

2.3. Anti-IBV immunohistochemistry

Formalin-fixed, paraffin-embedded 4-5 μm sections of CAM were mounted on glass slides and subsequently deparaffinized and rehydrated in alcohol series. Next, the sections were subjected to endogenous peroxidase inactivation by incubating slides in 1% hydrogen peroxide in methanol for 30 min at room temperature (RT). Antigen retrieval was performed by boiling the slides for 10 min in preheated 10 mM Tris-EDTA at pH 9.0. Wash buffer was composed of 1× Normal Antibody Diluent (ScyTek Laboratories, USA) containing 0.1% Tween-20. IBV antigens were detected by incubating the tissue sections at RT for 60 min with nucleocapsid protein-specific mouse monoclonal antibody (1:100 dilution; clone Ch/IBV 48.4; Prionics, The Netherlands). Antibody binding was detected by Dako Envision HRPO labeled polymer anti-mouse (Dako, USA). The staining was visualized by 3,3′-diaminobenzidine (DAB). Slides were counterstained with Hematoxylin and mounted with Eukitt® (Kindler, Germany). The presence of viral antigens was assessed by light microscopy and captured using a charge-coupled device (CCD) camera and an Olympus BX41 microscope linked to CellB̂ imaging software (Soft Imaging Solutions GmbH, Germany).

2.4. Genes and expression vectors

Sequences of IBV-M41 (accession number AY851295) and -Beaudette CK (accession number AJ311317) were obtained from the National Center for Biotechnology Information (NCBI) GenBank (http://www.ncbi.nlm.nih.gov/genbank/). Expression vectors encoding codon-optimized S1 genes of M41 (M.S1) or Beaudette (B.S1) were previously described (Wickramasinghe et al., 2011). Sequences encoding the S2 ectodomain part of the spike (comprising aa 539 to 1091 for both M41 and Beaudette) were codon-optimized for human expression and synthesized (Genscript, Piscataway, NJ, USA). At the S1/S2 border, the furin cleavage site sequence RRFRR was replaced by GGGVP, allowing the production of full length S ectodomains. The codon-optimized S2 sequences were subsequently cloned into the pCD5 vector containing the S1 domain of M41 or Beaudette using *Kpn*I and *Pac*I restriction enzymes, generating pCD5-B.ED and pCD5-M.ED. The S ectodomain genes were preceded by an N-terminal CD5 signal sequence and followed by sequences coding for a C-terminal

Table 1
Overview of the IBV spike constructs and their characteristics.

Abbreviation	Description	Schematic outline	Sequence aa 533–538	ProP score S1/S2	Sequence aa 686–691	ProP score 2nd
	Beaudette full length spike protein		RRFRR/S	0.779	SRRKR/S	0.833
	M41 full length spike protein		RRFRR/S	0.779	SPRRRS	0.331
B.S1	Beaudette S1		Not present	×	Not present	×
M.S1	M41 S1		Not present	×	Not present	×
B.ED	Beaudette ectodomain		GGGVPS	0	SRRKR/S	0.833
B.ED^{*cl}	Beaudette ectodomain; 2nd furin cleavage site knockout		GGGVPS	0	SHRKHS	0.102
B.ED^{*M41}	Beaudette ectodomain; 2nd cleavage site mutation M41		GGGVPS	0	SPRRRS	0.331
M.ED	M41 ectodomain		GGGVPS	0	SPRRRS	0.331
M.S1-B.S2^{*cl}	M41 S1 – Beaudette S2; 2nd furin cleavage site knockout		GGGVPS	0	SHRKHS	0.102
B.S1-M.S2	Beaudette S1 – M41 S2		GGGVPS	0	SPRRRS	0.331

Sequences with ProP scores less than 0.5 are considered not to be cleaved by furin.
/ indicates site of furin cleavage.
www.cbs.dtu.dk/services/ProP.

artificial GCN4 trimerization motif and Strep-tag II for detection and purification of proteins, as described before (Wickramasinghe et al., 2011). In addition, we generated two B.ED mutants, one in which the sequence encoding the second furin cleavage site SRRKR/S was mutated into a sequence predicted not to be cleaved (Table 1), but composed of the heparin-binding consensus SHRKHS (aa 686–691), resulting in B.ED^{*cl}, and one in which this site was replaced with the corresponding sequence of M41 SPRRRS, resulting in B.ED^{*M41} (Table 1). Expression vectors encoding chimeric S ectodomains were generated by cloning the S2 domains into the pCD5-S1 encoding plasmids with the reciprocal strain using *Kpn*I and *Pac*I restriction enzymes, for expression of proteins B.S1-M.S2 and M.S1-B.S2 (Table 1).

2.5. Production of recombinant spike proteins and purification

Spike proteins were produced in mammalian HEK293T cells as described before (Wickramasinghe et al., 2011). For spike protein production from avian cells, chicken fibroblast DF1 cells at 60% confluence were transfected with pCD5-B.S1 or pCD5-M.S1 using NanoJuice (Novagen). To this end, NanoJuice Reagent and Booster were mixed in 1:1 ratio (5 μl each per 35 cm^2 culture surface area) before adding them to pre-warmed DMEM and incubation for 5 min at RT. Plasmid DNA (3.5 μg per 35 cm^2 culture surface area) was added and incubated at RT for 15 min before adding it onto DF1 cells. After 24 h transfection, the transfection mixture was replaced by expression medium, as described for HEK293T cells (Wickramasinghe et al., 2011). The supernatants were harvested 9 days post-transfection, and the proteins were purified using Strep-Tactin Sepharose beads according to the manufacturer's protocols (IBA GmbH). The protein concentrations were determined by Qubit® 2.0 fluorometer (Invitrogen).

2.6. Western blot and PNGaseF treatment

The expression and purification of the IBV spike proteins were confirmed by sodium dodecyl sulfate-polyacrylamide gel electrophoresis (SDS-PAGE) followed by Western blotting using horseradish peroxidase (HRPO)-conjugated Strep-Tactin (IBA GmbH). Where indicated, the spike proteins were treated with N-glycosidase F (PNGase F; New England Biolabs Inc.) prior to electrophoresis according to the manufacturer's procedures to remove oligosaccharide side chains.

2.7. Prediction of cleavage by furin

To predict cleavage at the proposed second furin-type cleavage site, sequences were analyzed using the ProP 1.0 server (http://www.cbs.dtu.dk/services/ProP/). Prediction scores above 0.5 indicate that the residue is likely followed by an R-K propeptide cleavage site. The ProP scores for wild type and mutant sequences are shown in Table 1.

2.8. Spike histochemistry, tissue treatment with soluble heparin and VCNA

Sections (4–5 μm thick) of formalin-fixed, paraffin-embedded tissues from a 6-week-old male broiler chicken and an 11-day old SPF chicken embryo were used to study the binding of spike glycoproteins as described previously (Wickramasinghe et al., 2011). To study the dependence of the binding of spike ectodomains on heparan sulfate and sialic acids, tissue slides were pre-incubated overnight with 1 and 10 mg/ml of soluble sodium heparin (Sigma–Aldrich, GmBH) at 4 °C, or with 1 mU neuraminidase from Vibrio cholera (VCNA) (Roche) at 37 °C, respectively, before performing spike histochemistry.

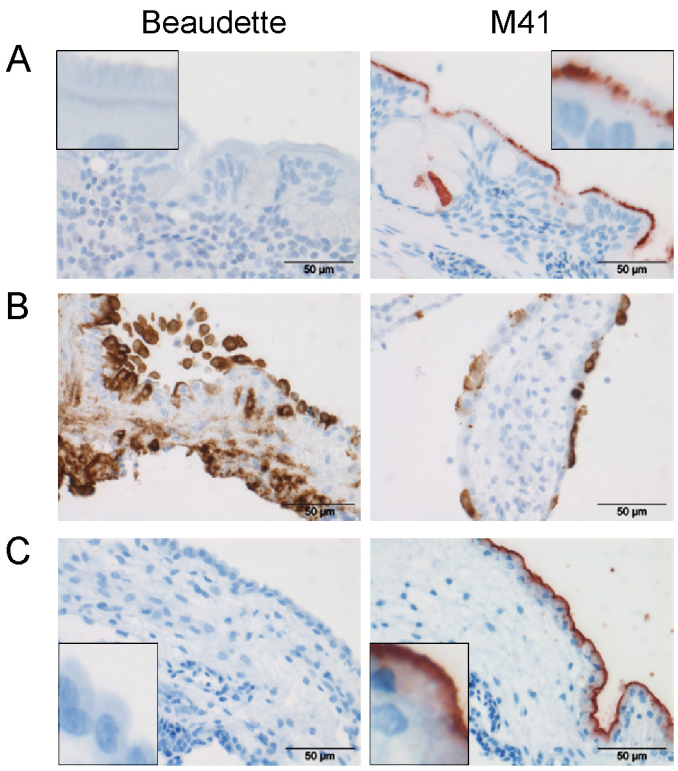

Fig. 1. Spike and anti-IBV histochemistry on chicken tissues. Chicken trachea (A) and CAM derived from embryonated eggs (C) were used for spike histochemistry. Beaudette S1 (B.S1) and M41 S1 (M.S1) proteins (5 μg) expressed from HEK293T cells were applied to each tissue section and spike histochemistry was performed as described before (Wickramasinghe et al., 2011); (B) immunohistochemistry using anti-IBV nucleocapsid monoclonal antibody 48.4 was performed on CAM isolated from embryonated eggs 2 days after inoculation with IBV Beaudette and M41 as described in Section 2.

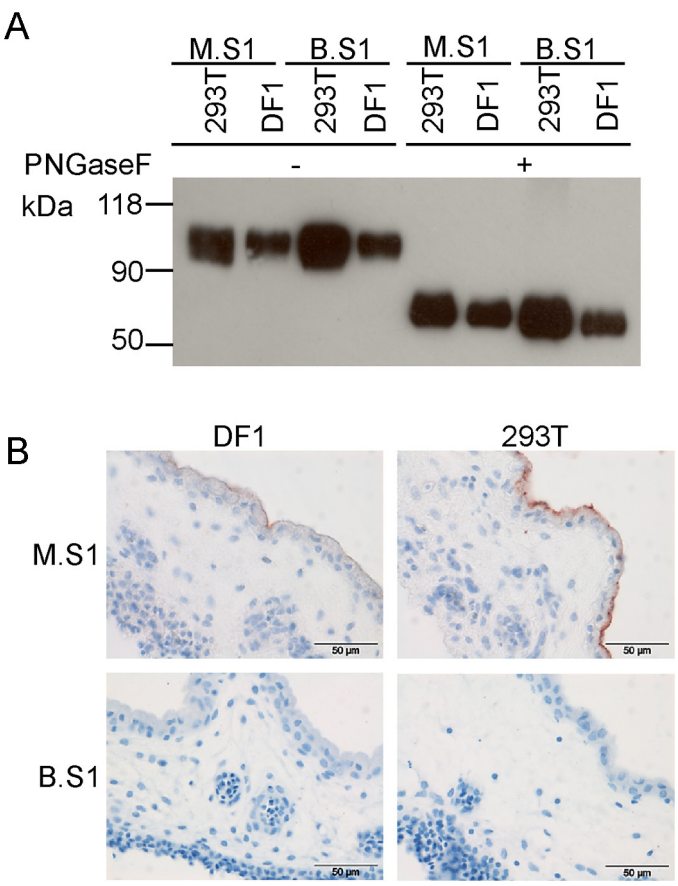

Fig. 2. Expression of recombinant IBV S1 proteins produced in mammalian and chicken cells and spike histochemistry on chicken tissues. (A) S1 proteins expressed in human HEK293T and chicken DF1 cells were purified from the culture media. The proteins were analyzed by SDS-PAGE followed by Western blot using Strep-Tactin; when indicated the samples were treated with PNGaseF prior to electrophoresis; (B) spike histochemistry on CAM tissue using similar amounts of each of the S1 proteins.

3. Results

3.1. Recombinant Beaudette S1 does not display detectable binding to virus-susceptible CAM tissue

We confirmed our previous observations (Wickramasinghe et al., 2011) that recombinant S1 protein of the embryo- and cell culture-adapted IBV strain Beaudette (B.S1) did not show binding to the chicken trachea in our spike histochemistry assay, while in contrast, the S1 of the virulent M41 strain (M.S1) displayed clear binding to the base of the cilia and goblet cells of the trachea (Fig. 1A). To exclude that the lack of binding of B.S1 was due to the absence of appropriate receptors on this tissue, we next selected embryonic CAM tissues, reported to support infection and replication of both IBV Beaudette and M41. Indeed, after inoculating eggs on day 11 of embryonation with IBV-M41 or -Beaudette, viral antigens could readily be detected in both allantoic and chorionic epithelium of the CAM when stained with antibody for the nucleocapsid protein at 2 days post-inoculation (Fig. 1B). As expected, Beaudette-infected embryos even displayed a higher number of infected cells than M41-infected embryos when using the same inoculation titer, due to the adaptation of Beaudette to embryos. Spike histochemistry performed on CAM sections of non-infected 11-day-old embryonated eggs showed, however, that B.S1 was not able to bind to these tissues, while M.S1 displayed clear binding to the allantoic membrane (Fig. 1C). Taken together, these results suggest that the lack of binding of Beaudette S1 is not due to lack of attachment factors on the host tissue, but is rather an intrinsic feature of the recombinant Beaudette S1 protein.

3.2. Recombinant Beaudette S1 expressed from avian cells does not bind to CAM

Recombinant spike proteins used in our assay are produced in a well-established mammalian expression system in human HEK 293T cells. To exclude that the lack of binding of B.S1 to CAM and trachea is due to yet unrevealed differences in protein glycosylation between mammalian cells and the natural avian host, we next produced Beaudette S1 proteins from chicken DF1 cells. To this end, transfection conditions were optimized for this particular cell type and soluble proteins collected from the supernatant of these cells were purified (Wickramasinghe et al., 2011) and analyzed by Western blot. Recombinant M.S1 and B.S1 produced in DF1 cells migrated with an electrophoretic mobility comparable to proteins produced in 293T cells (Fig. 2A). Although differences in glycosylation cannot be excluded, S1 proteins produced in avian cells are, like those produced in human cells, highly glycosylated, as removal of the N-linked glycans with PNGaseF increased the electrophoretic mobility of all S1 proteins to around 70 kDa. Of note is that the amount of soluble protein produced in avian cells was repeatedly less than that produced in mammalian cells. This might be caused by the less robust expression of recombinant proteins in avian cells, or due to slight differences in preferred codon-usage of avian and mammalian cells.

Spike histochemistry using similar amounts of recombinant proteins showed, however, no appreciable staining of the CAM when B.S1 produced in avian DF1 cells were applied. For M.S1

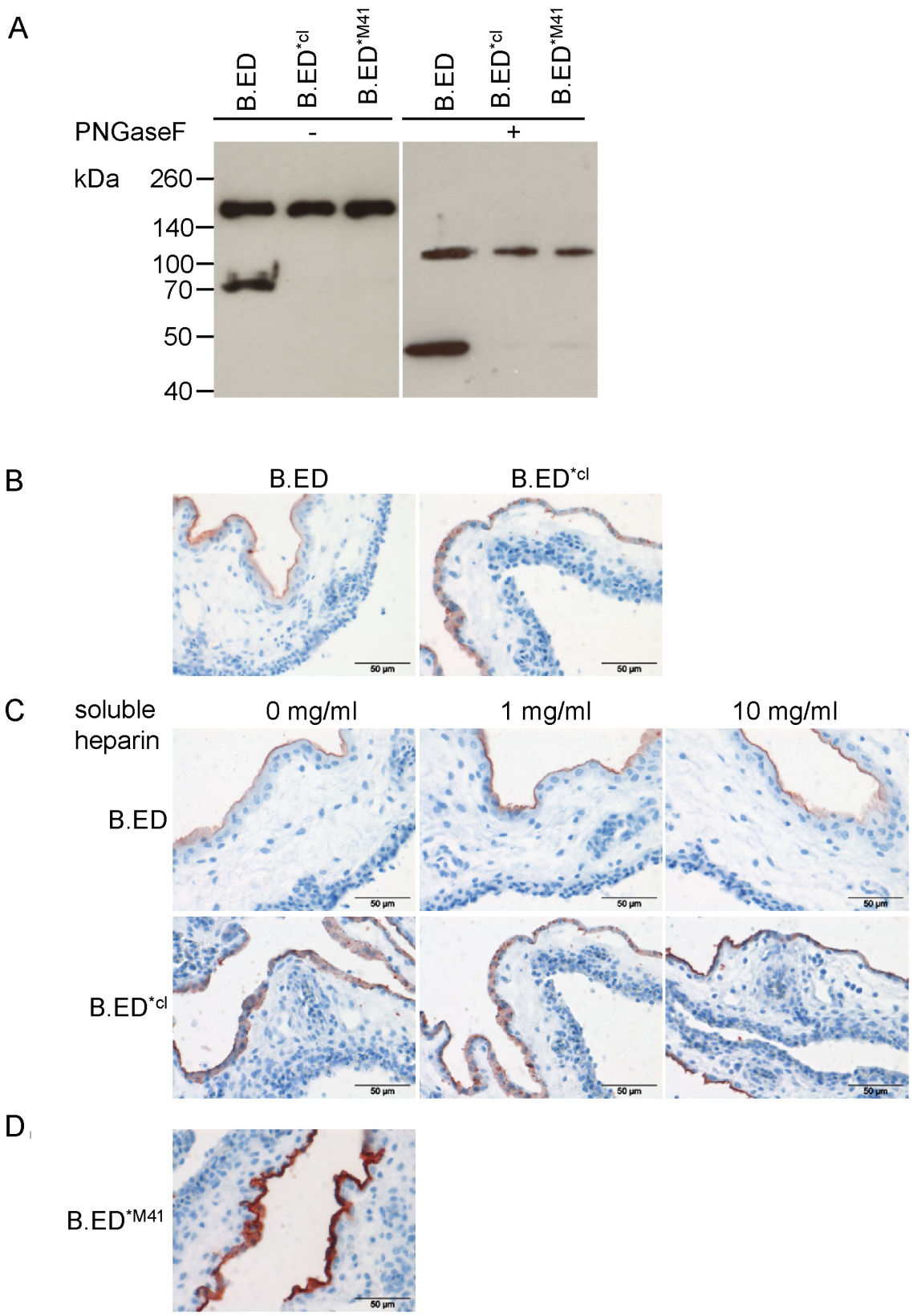

Fig. 3. Expression of recombinant IBV Beaudette spike ectodomains and analysis of binding to CAM. (A) Soluble Beaudette spike ectodomains were produced in HEK293T cells, purified, and subsequently analyzed by Western blot using Strep-Tactin; when indicated the samples were treated with PNGaseF prior to electrophoresis; (B/C/D) Spike histochemistry was performed on CAM tissues using 9 μg Strep-Tactin-precomplexed B.ED and mutants thereof before (B and D) or after (C) pre-incubating the tissues with various concentrations of soluble heparin.

we observed that the level of binding of S1 proteins produced in avian cells was slightly less than that produced in mammalian cells (Fig. 2B), for reasons that are currently unknown. Threefold increase in the amount of both mammalian and avian-produced B.S1 protein did not result in detectable binding to CAM (data not shown). Taken together, the previously observed lack of binding of B.S1 to CAM is likely not due to potential differences in glycosylation or other yet unrecognized differences between proteins produced in human and avian cells. Likely, other viral protein domains contribute to the binding of Beaudette to susceptible cells, by providing either an additional binding site or increasing the affinity of the S1 domain.

3.3. The S2 domain, but not HS binding site, is required for gain of binding of Beaudette spike to susceptible tissues

Currently, all evidence points toward a sole contribution for the viral glycoprotein spike in coronaviral attachment. While the S1 is generally assumed to contain the RBD, the C-terminal S2 domain might act in concert with S1 during entry and account for the extended host range, as was shown for a murine hepatitis virus (MHV) strain with extended tropism (de Haan et al., 2006). In addition, the S2 of Beaudette has a heparin-binding consensus XBBBXXB sequence (where X is a hydropathic amino acid and B is a basic residue, as previously defined by Cardin and Weintraub, 1989). This sequence has earlier been proposed to bind to HS on the cell surface and thereby be responsible for the extended tropism of Beaudette (Madu et al., 2007). To investigate the role of the Beaudette S2 domain in attachment, we extended our Beaudette S1-encoding constructs to now comprise the complete spike ectodomain, but lacking the non-exposed transmembrane and cytoplasmic domains. To be able to generate full-length soluble spike ectodomains, we decided to mutate the furin cleavage site (aa 533–538) in Beaudette spike from RRFRR/S to GGGVPS (Table 1) as cleavage between S1 and S2 is not important for binding, but rather affects downstream events in the infection (Yamada and Liu, 2009). In Beaudette S2, however, the putative HS-binding sequence overlaps with a second furin cleavage site (aa 686–691; SRRKR/S) (Yamada and Liu, 2009). To allow to study the role of this sequence in binding we decided to generate two versions of the Beaudette spike ectodomain: one containing the wild type Beaudette sequence SRRRR/S at the secondary cleavage site (B.ED), and one in which this sequence was mutated to SHRKHS, resulting in loss of predicted furin cleavage (Table 1, compare ProP scores), while retaining the heparin-binding consensus sequence (B.ED^{*cl}). Codon-optimized sequences were cloned into our expression vector such that they were again preceded with a CD5 signal sequence and followed by a trimerization domain and a Streptag for purification and analysis purposes. Recombinant proteins were expressed in 293T cells and analyzed by Western blot (Fig. 3A). While for B.ED^{*cl} one protein band migrating at approximately 200 kDa was observed, an additional protein band was observed for B.ED migrating at around 70 kDa. As detection is based on the presence of the Streptag, these proteins likely represent the full-length ectodomain and the C-terminal domain after furin cleavage, respectively. These results indicate that recombinantly produced Beaudette-ED is partially cleaved during production, while cleavage is abrogated in the mutant B.ED^{*cl}. PNGaseF treatment showed that the spike ectodomains migrate around the expected 130 kDa, confirming that these proteins are, as previously observed (Yamada et al., 2009) and like the S1, highly glycosylated. For B.ED, the observed additional band after PNGaseF treatment migrating around 47 kDa corresponds with the expected size of the C-terminal domain with Streptag after furin cleavage.

Next, we analyzed the ability of B.ED and B.ED^{*cl} to bind to CAM tissue. Spike ectodomain was again precomplexed with Strep-Tactin, now using 9 μg of protein per slide (resulting in equimolar amounts of proteins as used for B.S1 in Fig. 2). In spike histochemistry we observed that both B.ED and B.ED^{*cl} stained the allantoic membrane of the CAM (Fig. 3B), indicating that extension of S1 with sequences from the S2 ectodomain was sufficient to gain binding of the spike to susceptible tissues. It seems most likely that the full-length soluble ectodomains of B.ED and B.ED^{*cl} are responsible for the ultimate binding to the tissue, although we cannot exclude a particular contribution of the smaller C-terminal domain if still complexed with full length ectodomains. To investigate whether the binding of these proteins was due to the presence of the HS binding site in S2, we blocked CAM tissues with soluble heparin before applying recombinant B.ED and B.ED^{*cl} proteins. No reduction in binding was observed when applying either 1 or 10 mg/ml soluble heparin (Fig. 3C), suggesting that HS binding is not required for binding of Beaudette spikes to susceptible tissues. To confirm this, we generated a mutant recombinant Beaudette spike ectodomain, in which the heparin consensus sequence was changed into the corresponding sequence of M41 at that position (aa 686–691, SPRRRS; Table 1). The resulting protein, B.ED^{*M41} lacking both the consensus HS binding site and the furin cleavage site was expressed from 293T cells as full length ectodomain (Fig. 3B), and had the ability to bind to the allantoic epithelium of CAM tissues (Fig. 3D). Interestingly, this mutant displayed even greater binding to the CAM; the reason for this remains unclear. In conclusion, the Beaudette S2 ectodomain, but not the proposed HS binding site, is required for attachment of spike to susceptible chicken tissues.

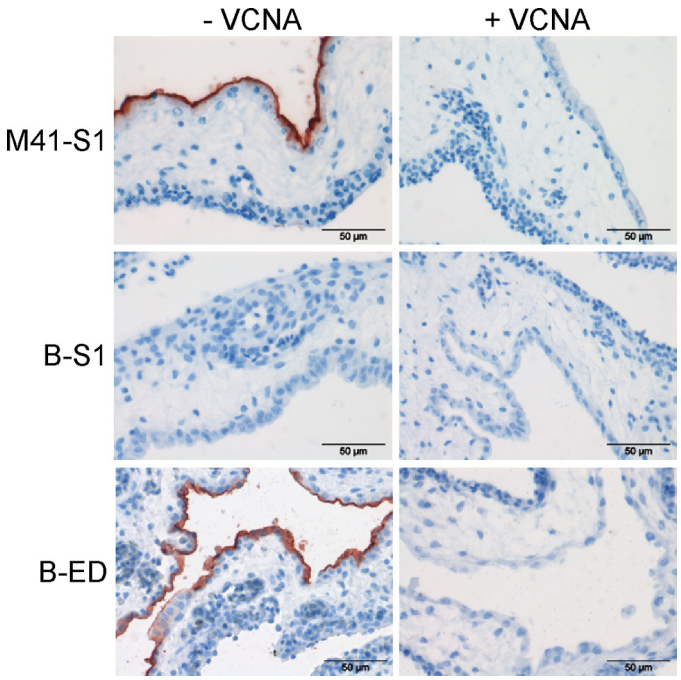

Fig. 4. Binding of recombinant Beaudette ectodomain depends on sialic acids. CAM tissues were pretreated with PBS (-VCNA) or PBS with VCNA (+VCNA) prior to spike histochemistry.

3.4. Binding of Beaudette spike ectodomain depends on sialic acids

Previously, we showed that attachment of the S1 protein of M41 is dependent on alpha-2,3-linked sialic acids (Wickramasinghe et al., 2011). In order to elucidate whether Beaudette spike ectodomain binding also relies on the interaction with sialic acids present on host cells, we pretreated the cells with Vibrio cholera neuraminidase (VCNA) before applying the spike proteins onto the tissues. As a control, we included M.S1 (Fig. 4). Spike histochemistry revealed that the binding of B.ED was completely lost after VCNA

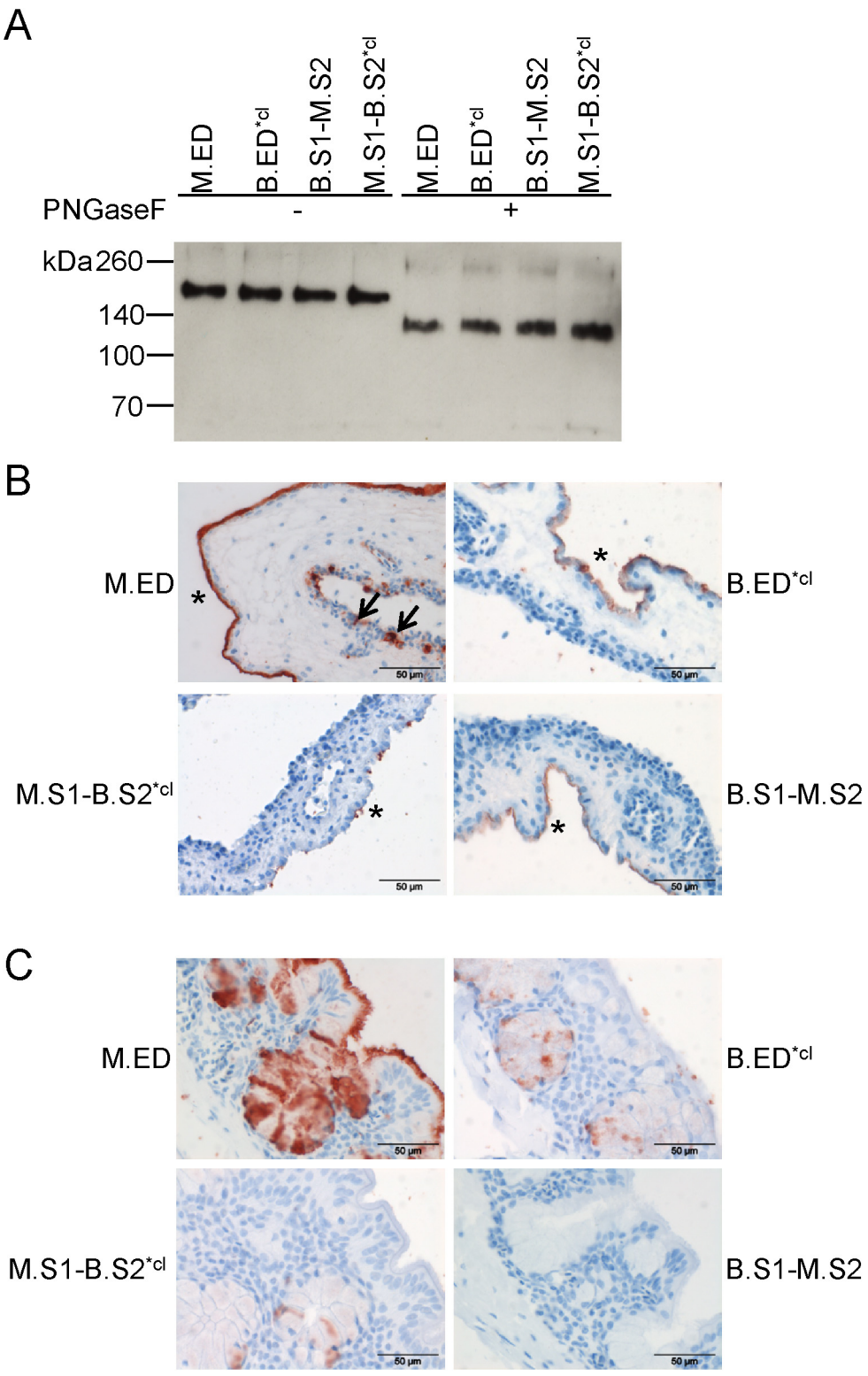

Fig. 5. Expression of chimeric recombinant IBV spike ectodomains and analysis of binding to CAM. (A) Soluble spike ectodomains were produced in HEK293T cells, purified, and subsequently analyzed by Western blot using Strep-Tactin; (B/C) Spike histochemistry was performed on CAM (B) and chicken trachea (C) using 9 μg chimeric recombinant spike proteins precomplexed with Strep-Tactin. * indicates the allantoic membrane; arrows indicate staining of the chorionic membrane.

treatment, showing that also the Beaudette spike requires sialic acids for its attachment to the cell surface of susceptible cells. These results are in agreement with previous observations that sialic acids serve as receptor determinants for Beaudette on respiratory tract epithelium and primary chicken kidney cells (Abd El Rahman et al., 2009; Winter et al., 2006, 2008).

3.5. The S2 domain likely does not contain an additional independent binding site, but rather contributes to the avidity of spike attachment

Whether the observed gain of binding of Beaudette spike is due to the presence of an additional receptor-binding domain in S2

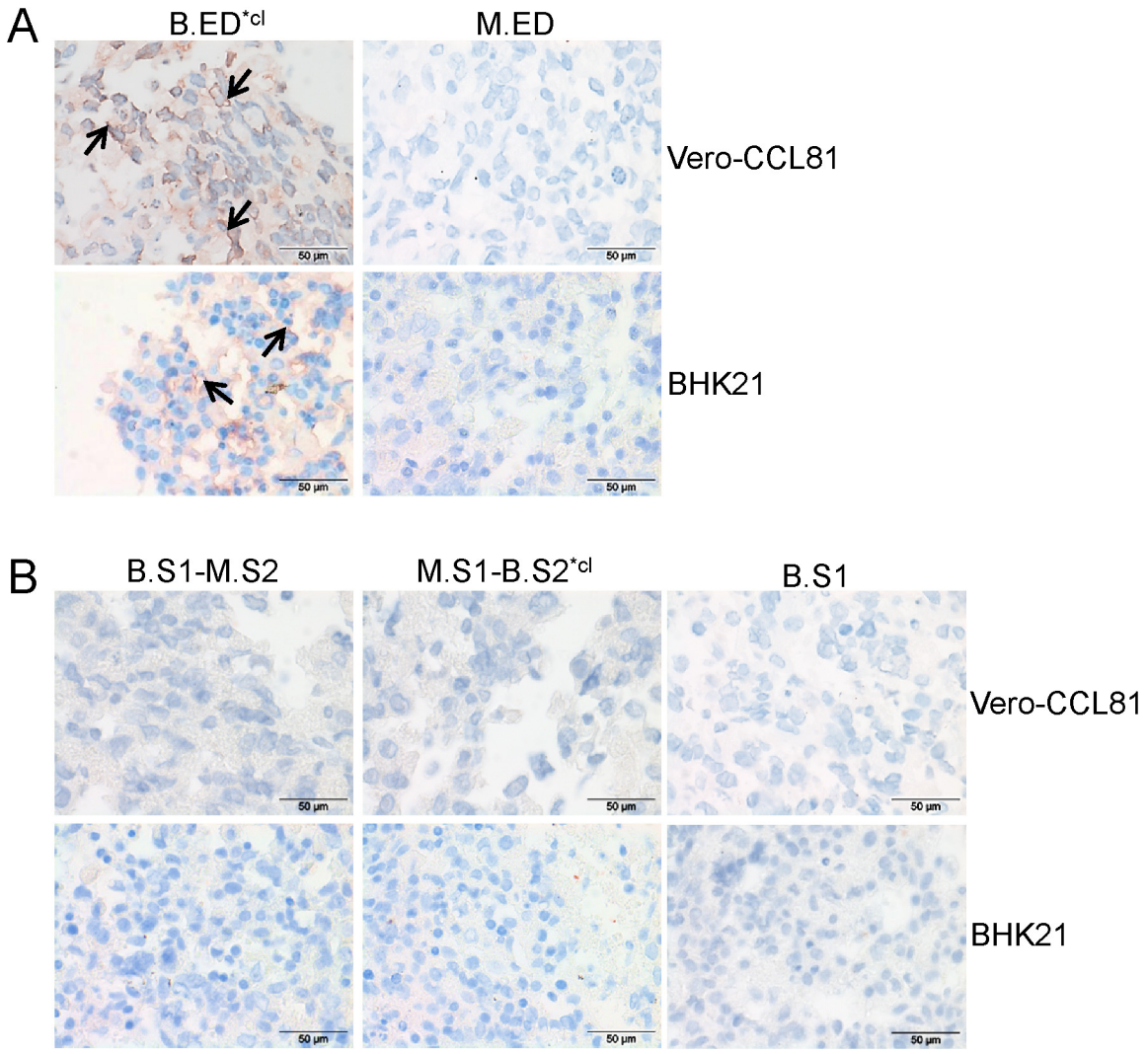

Fig. 6. Binding of recombinant IBV spike ectodomains to mammalian cell cultures. Spike histochemistry was performed on pelleted cells of Vero-CCL81 and BHK-21 cultures using Strep-Tactin precomplexed spike ectodomains of Beaudette and M41 (A) and chimeras thereof (B). Arrows point to examples of cell membrane staining.

or whether this region stabilizes the conformation of S1 resulting in increased avidity and thus detectable binding in our assay is unknown. To elucidate whether the S2 domain harbors an additional attachment site, we first separately cloned the S2 part of the ectodomain (aa 539–1091) of Beaudette in our expression vector, lacking S1. Unfortunately, no recombinant proteins could be detected in the cell culture supernatant of HEK293T cells transfected with the resulting plasmid (data not shown), suggesting that the S2 ectodomain could not fold independently from the S1 domain.

As an alternative approach to get a hint of the contribution of S1 and S2 in attachment, we generated chimeric spike ectodomain proteins, composed of the S1 domain of M41 and the S2 domain of Beaudette or the reciprocal. For proteins containing the S2 domain of Beaudette we used the BS2^{*cl} sequence to prevent subsequent cleavage. As control proteins we produced soluble full length M41 (M.ED) and Beaudette (B.ED^{*cl}) ectodomains. The proteins were produced in 293T cells and Western blot analysis using Strep-Tactin showed that all proteins could be expressed and had the expected mobility in SDS-PAGE gel (Fig. 5A). In spike histochemistry, M.ED interestingly displayed not only binding to the allantoic, but also to the chorionic membrane of the CAM (Fig. 5B). In particular, the binding resembled the sites of replication of IBV in the CAM after infection most closely (Fig. 1B). Again, the extended binding of M.ED compared to M.S1 (Fig. 1C) could be due to the presence of an additional binding site in S2 or a concerted action between S1 and S2 thereby increasing the binding avidity. To address this, we analyzed the binding of our chimeric proteins to CAM. For B.S1-M.S2 we observed a binding pattern comparable to that of B.ED^{*cl} (Fig. 5B). More specifically, binding was observed to the allantoic epithelium of the CAM, but with rather low avidity. In addition, M.S1-B.S2^{*cl} demonstrated slightly reduced binding compared to M.S1, suggesting that the gain of binding of Beaudette and the extended binding of M41 is probably not due to the presence of an additional receptor-binding site in S2. The presence of an additional binding site for glycans in M.S2 was excluded by glycan array analysis using M.ED, where we observed a similar preference for alpha-2,3-linked sialic acids as for M.S1 (data not shown). The observed increased affinity for these carbohydrate structures in glycan array was in line with the increased levels of binding in spike histochemistry.

Taken together, our data suggest that the presence of S2 increases the avidity of S1 resulting in detectable binding of these spikes to susceptible tissue. Although not required for binding to CAM per se, it seems that combinations of S1 and S2 originating from the same viral origin work best. This was confirmed when performing spike histochemistry on chicken trachea tissues (Fig. 5C). M.ED displayed strong binding to both goblet cells and ciliated epithelium, but also B.ED^{*cl} and B.ED (not shown) had the ability

to bind to this tissue. In contrast to what was observed for CAM, the combination of B.S1 and M.S2 was not sufficient for binding to trachea (Fig. 5C), suggesting that a concerted action between Beaudette S1 and S2 in combination with the presence of particular host surface molecules determines the range of attachment to tissues.

3.6. Beaudette spike ectodomain displays extended attachment for mammalian cell lines

Finally, we elucidated whether the extended host range of IBV Beaudette, that is, its ability to infect mammalian cell cultures, is also reflected by the attachment pattern of the spike ED. To this end, we performed spike histochemistry on formalin-fixed, paraffin-embedded Vero-CCL81 and BHK-21 cells, known to be susceptible to Beaudette. Our results show that B.ED^{*cl}, but not M.ED, binds to the cell surface of these culture cells (Fig. 6A). The rather limited signal of binding to culture cells compared to chicken tissues might be due to a lower expression of attachment factors on these cells, which likely reduces the sensitivity of the assay. B.S1 alone did not have the ability to bind to these cells (Fig. 6B), nor the chimeric ED proteins with Beaudette S1 or S2 fused to M41 S2 or S1, respectively, even when using 5-fold higher protein concentration. Taken together, our results indicate that specific sequences present in both Beaudette S1 and S2 contribute to the mammalian cell tropism of Beaudette. Where these particular domains in these subunits are situated and how they both contribute to the extended host tropism will require further investigation.

4. Discussion

Previously we showed that while the S1 domain of the spike of the virulent IBV strain M41 was sufficient for attachment to chicken respiratory tract tissues, the same spike subunit of the embryo-and cell culture adapted Beaudette was unable to bind. We have now demonstrated that this lack of appreciable binding was apparently not due to the absence of attachment factors on host tissue or due to its expression from mammalian cells, but that the combined presence of the S1 and the S2 subunits of the spike ectodomain were essential for attachment. Results of binding experiments using chimeric spike proteins further suggest that the S2 subunit does not contain an additional independent binding site, but rather works together with S1 to acquire binding of the spike to host cells. As only combined S1 and S2 sequences of Beaudette, but not M41, resulted in gain of binding to mammalian cells, this suggests that Beaudette S1 and S2 communicate to establish the first critical step in the extended host tropism of the virus. It might well be that particular sequences in S2 contribute to the higher order structure, stability, or exposure of the receptor binding domain present in the viral attachment protein spike.

Many viruses that have been serially passaged, or isolated from persistently infected cells, have acquired the ability to infect previously non-susceptible cells. For coronaviruses, the extended host range of such viruses has not only been described for IBV (Otsuki et al., 1979; Tay et al., 2012; Yamada et al., 2009), but also for MHV (Baric et al., 1997, 1999; McRoy and Baric, 2008; Sawicki et al., 1995; Schickli et al., 1997, 1998). Cells persistently infected with MHV and passaged multiple times generated a virus that gained the ability to enter cells independent of its natural protein receptor CEACAM, but rather use heparan sulfate, explaining their extended cell tropism (de Haan et al., 2005). HS is a well-known co-factor for viral attachment to host cells (Liu and Thorp, 2002), and has previously been implicated in the extended host range of IBV Beaudette (Madu et al., 2007). Blocking of Beaudette infection in mammalian cells required, however, rather high concentrations of soluble heparin (Madu et al., 2007). In our study, we observed no inhibition of attachment of the Beaudette spike to relevant tissues in the presence of soluble heparin as blocking reagent. The lack of involvement of HS in the attachment and the subsequent extended host range of Beaudette is further confirmed upon mutation of the heparin consensus sequence into the corresponding sequence of IBV-M41 with regard to spike binding (this paper) and subsequent entry (Yamada and Liu, 2009), and the observed enhancing effect of pretreatment of Vero cells with heparinase I on infection (unpublished data cited in Yamada and Liu, 2009).

Adaptation of IBV strains to embryonated eggs, and in particular Beaudette to Vero cells (Fang et al., 2005; Shen et al., 2004) is accompanied with accumulating mutations in the spike gene. While it is generally assumed that the RBD of IBV is located in S1, and thus that sequence differences between S1s of Beaudette and M41 contribute to host range, the S1 protein of Beaudette alone was not sufficient for binding to chicken trachea (Wickramasinghe et al., 2011), embryonic CAM tissue and mammalian cell lines (this study). Appreciable binding of the Beaudette spike required both the S1 domain and S2 ectodomain, while the extension of M41 S1 with the S2 ectodomain resulted in higher avidity and extended specificity of binding to chicken CAM and trachea tissues. Chimeras showed that both S1 and S2 need to be from the same origin to support the increase in binding (Fig. 5B and C) and the extended host range of Beaudette in particular (Fig. 6A and B). So while Beaudette and M41 spike ectodomains have over 96% amino acid similarity, likely differences not only in the yet-to-be-mapped RBDs, but also other parts of the spike may affect the binding. Although we cannot completely rule out the presence of an additional attachment site in S2, we believe that the combined presence of S1 and S2 contributes to the attachment, either by altering the stability or the conformation of the spike, resulting in increased binding avidity of the, yet to be identified, RBD in S1. This hypothesis is supported by our unpublished observation that the M41 ectodomain bound to a comparable set of alpha-2,3-sialic acid containing glycans as M41 S1 (Wickramasinghe et al., 2011), albeit with a higher avidity. Unfortunately, glycan array analysis for the Beaudette spike ectodomain did not reveal binding to any particular glycan, which might be due to its relatively low avidity in binding compared to M41 (Fig. 5B and C). Nevertheless, we clearly demonstrate that attachment of the Beaudette spike ectodomain to host cells requires sialic acids, as binding is precluded when CAM tissue is pretreated with neuraminidase (Fig. 4). This is in line with previous reports showing that the embryo- and cell culture adapted IBV strain, like other IBV strains, requires sialic acids for infection (Abd El Rahman et al., 2009; Winter et al., 2006, 2008).

In coronavirus infections, when processes of virus attachment and entry cannot be distinguished from each other, a concerted action between S1 and S2 has been observed. For example, the extended host range of MHV strains often requires a combination of mutations in S1 and S2 (de Haan et al., 2006; Navas-Martin et al., 2005; Saeki et al., 1997; Schickli et al., 2004; Thackray and Holmes, 2004). When elucidated in more detail, the communication between these regions was particularly contributing to virus-cell fusion and spread of progeny virus. Also for the human coronavirus NL-63, the S2 domain affected the structure and stability of the spike, ultimately required to drive fusion-activating events after binding to the host cell receptor (Zheng et al., 2006). Similarly, for IBV it has been shown that mutations gained during cell passage contributed to increased ability to promote cell-cell fusion (Yamada et al., 2009). In particular, one amino acid change (L857F) converted a non-fusogenic S protein to a fusogenic one, but compensatory mutations in the S1 domain were also required to rescue the cell-cell fusion activity. Our study, however, suggests that S2 not only contributes to virus-cell fusion, but that it might also be crucial for the very first step in virus infection. Whether differences in the

metastability of spike ectodomains of Beaudette and M41 account to some extent for the differences in cell tropism, as suggested for MHV (de Haan et al., 2006; Tsai et al., 2003), or whether several domains in the spike are required for binding or to form higher order structures to expose the RBD remains to be seen.

Many cellular factors are involved in the subsequent steps of the IBV replication cycle (reviewed in Zhong et al., 2012). After attachment, the virus is internalized and the spike is activated, followed by release of the viral genome in the cytoplasm. Although cleavage of the spike between S1/S2 is not necessary for attachment, it promotes the infectivity of IBV in cells (Yamada and Liu, 2009). In contrast, the second furin cleavage site in the Beaudette spike is required for furin dependent entry and syncytium formation (Yamada and Liu, 2009). This correlates with the observation that a productive Beaudette infection is associated with cellular furin abundance in the host cell (Tay et al., 2012). Interestingly, part of this second furin recognition sequence motif (XXXR/S) is present in many coronaviruses, including M41, and has been proposed to be a common mechanism for entry of coronaviruses into cells (Yamada and Liu, 2009).

In conclusion, the S1 subunit of IBV Beaudette spike is not sufficient for binding to host tissues, while the full length Beaudette spike ectodomain gained the ability to bind to embryonic and 6-week-old chicken tissues, as well as mammalian cells known to be susceptible to the virus. Based on our current results, we hypothesize that the interplay between the S1 and S2 subunits of spikes from the same viral origin ultimately determine the avidity and specificity of virus attachment and thus viral tropism.

Acknowledgements

We would like to thank Vicky van Santen for critical reading of the manuscript. MHV is financially supported by a MEERVOUD grant from the Netherlands Organization for Scientific Research (836.12.012).

References

Abd El Rahman, S., El-Kenawy, A.A., Neumann, U., Herrler, G., Winter, C., 2009. Comparative analysis of the sialic acid binding activity and the tropism for the respiratory epithelium of four different strains of avian infectious bronchitis virus. Avian Pathol. 38, 41–45.

Adams, M.J., Carstens, E.B., 2012. Ratification vote on taxonomic proposals to the International Committee on Taxonomy of Viruses (2012). Arch. Virol. 157, 1411–1422.

Armesto, M., Evans, S., Cavanagh, D., Abu-Median, A.B., Keep, S., Britton, P., 2011. A recombinant avian infectious bronchitis virus expressing a heterologous spike gene belonging to the 4/91 serotype. PLoS One 6, e24352.

Baric, R.S., Sullivan, E., Hensley, L., Yount, B., Chen, W., 1999. Persistent infection promotes cross-species transmissibility of mouse hepatitis virus. J. Virol. 73, 638–649.

Baric, R.S., Yount, B., Hensley, L., Peel, S.A., Chen, W., 1997. Episodic evolution mediates interspecies transfer of a murine coronavirus. J. Virol. 71, 1946–1955.

Beaudette, F.R., Hudson, C.B., 1937. Cultivation of the virus of infectious bronchitis. J. Am. Vet. Med. Assoc. 90, 51–58.

Belouzard, S., Millet, J.K., Licitra, B.N., Whittaker, G.R., 2012. Mechanisms of coronavirus cell entry mediated by the viral spike protein. Viruses 4, 1011–1033.

Bosch, B.J., van der Zee, R., de Haan, C.A., Rottier, P.J., 2003. The coronavirus spike protein is a class I virus fusion protein: structural and functional characterization of the fusion core complex. J. Virol. 77, 8801–8811.

Cardin, A.D., Weintraub, H.J., 1989. Molecular modeling of protein–glycosaminoglycan interactions. Arteriosclerosis 9, 21–32.

Casais, R., Dove, B., Cavanagh, D., Britton, P., 2003. Recombinant avian infectious bronchitis virus expressing a heterologous spike gene demonstrates that the spike protein is a determinant of cell tropism. J. Virol. 77, 9084–9089.

Cavanagh, D., Davis, P.J., Pappin, D.J., Binns, M.M., Boursnell, M.E., Brown, T.D., 1986. Coronavirus IBV: partial amino terminal sequencing of spike polypeptide S2 identifies the sequence Arg-Arg-Phe-Arg-Arg at the cleavage site of the spike precursor propolypeptide of IBV strains Beaudette and M41. Virus Res. 4, 133–143.

Cook, J.K., Darbyshire, J.H., Peters, R.W., 1976. Growth kinetic studies of avian infectious bronchitis virus in tracheal organ cultures. Res. Vet. Sci. 20, 348–349.

Cunningham, C.H., Spring, M.P., Nazerian, K., 1972. Replication of avian infectious bronchitis virus in African green monkey kidney cell line VERO. J. Gen. Virol. 16, 423–427.

de Haan, C.A., Li, Z., te Lintelo, E., Bosch, B.J., Haijema, B.J., Rottier, P.J., 2005. Murine coronavirus with an extended host range uses heparan sulfate as an entry receptor. J. Virol. 79, 14451–14456.

de Haan, C.A., Stadler, K., Godeke, G.J., Bosch, B.J., Rottier, P.J., 2004. Cleavage inhibition of the murine coronavirus spike protein by a furin-like enzyme affects cell–cell but not virus-cell fusion. J. Virol. 78, 6048–6054.

de Haan, C.A., Te Lintelo, E., Li, Z., Raaben, M., Wurdinger, T., Bosch, B.J., Rottier, P.J., 2006. Cooperative involvement of the S1 and S2 subunits of the murine coronavirus spike protein in receptor binding and extended host range. J. Virol. 80, 10909–10918.

Fang, S.G., Shen, S., Tay, F.P., Liu, D.X., 2005. Selection of and recombination between minor variants lead to the adaptation of an avian coronavirus to primate cells. Biochem. Biophys. Res. Commun. 336, 417–423.

Geilhausen, H.E., Ligon, F.B., Lukert, P.D., 1973. The pathogenesis of virulent and avirulent avian infectious bronchitis virus. Arch. Gesamte Virusforsch. 40, 285–290.

Graham, R.L., Baric, R.S., 2010. Recombination, reservoirs, and the modular spike: mechanisms of coronavirus cross-species transmission. J. Virol. 84, 3134–3146.

Guy, J.S., 2008. Isolation and propagation of coronaviruses in embryonated eggs. Methods Mol. Biol. 454, 109–117.

Heald-Sargent, T., Gallagher, T., 2012. Ready, set, fuse! The coronavirus spike protein and acquisition of fusion competence. Viruses 4, 557–580.

Hodgson, T., Casais, R., Dove, B., Britton, P., Cavanagh, D., 2004. Recombinant infectious bronchitis coronavirus Beaudette with the spike protein gene of the pathogenic M41 strain remains attenuated but induces protective immunity. J. Virol. 78, 13804–13811.

Jackwood, M.W., 2012. Review of infectious bronchitis virus around the world. Avian Dis. 56, 634–641.

Jackwood, M.W., Hilt, D.A., Callison, S.A., Lee, C.W., Plaza, H., Wade, E., 2001. Spike glycoprotein cleavage recognition site analysis of infectious bronchitis virus. Avian Dis. 45, 366–372.

Kawamura, H., Isogai, S., Tsubahara, H., 1961. Propagation of avian infections bronchitis virus in chicken kidney tissue culture. Natl. Inst. Anim. Health Q. 1, 190–198.

Liu, J., Thorp, S.C., 2002. Cell surface heparan sulfate and its roles in assisting viral infections. Med. Res. Rev. 22, 1–25.

Madu, I.G., Chu, V.C., Lee, H., Regan, A.D., Bauman, B.E., Whittaker, G.R., 2007. Heparan sulfate is a selective attachment factor for the avian coronavirus infectious bronchitis virus Beaudette. Avian Dis. 51, 45–51.

McRoy, W.C., Baric, R.S., 2008. Amino acid substitutions in the S2 subunit of mouse hepatitis virus variant V51 encode determinants of host range expansion. J. Virol. 82, 1414–1424.

Navas-Martin, S., Hingley, S.T., Weiss, S.R., 2005. Murine coronavirus evolution in vivo: functional compensation of a detrimental amino acid substitution in the receptor binding domain of the spike glycoprotein. J. Virol. 79, 7629–7640.

Otsuki, K., Noro, K., Yamamoto, H., Tsubokura, M., 1979. Studies on avian infectious bronchitis virus (IBV). II. Propagation of IBV in several cultured cells. Arch. Virol. 60, 115–122.

Saeki, K., Ohtsuka, N., Taguchi, F., 1997. Identification of spike protein residues of murine coronavirus responsible for receptor-binding activity by use of soluble receptor-resistant mutants. J. Virol. 71, 9024–9031.

Sawaguchi, K., Yachida, S., Aoyama, S., Takahashi, N., Iritani, Y., Hayashi, Y., 1985. Comparative use of direct organ cultures of infected chicken tracheas in isolating avian infectious bronchitis virus. Avian Dis. 29, 546–551.

Sawicki, S.G., Lu, J.H., Holmes, K.V., 1995. Persistent infection of cultured cells with mouse hepatitis virus (MHV) results from the epigenetic expression of the MHV receptor. J. Virol. 69, 5535–5543.

Schickli, J.H., Thackray, L.B., Sawicki, S.G., Holmes, K.V., 2004. The N-terminal region of the murine coronavirus spike glycoprotein is associated with the extended host range of viruses from persistently infected murine cells. J. Virol. 78, 9073–9083.

Schickli, J.H., Wentworth, D.E., Zelus, B.D., Holmes, K.V., Sawicki, S.G., 1998. Selection in persistently infected murine cells of an MHV-A59 variant with extended host range. Adv. Exp. Med. Biol. 440, 735–741.

Schickli, J.H., Zelus, B.D., Wentworth, D.E., Sawicki, S.G., Holmes, K.V., 1997. The murine coronavirus mouse hepatitis virus strain A59 from persistently infected murine cells exhibits an extended host range. J. Virol. 71, 9499–9507.

Shen, S., Law, Y.C., Liu, D.X., 2004. A single amino acid mutation in the spike protein of coronavirus infectious bronchitis virus hampers its maturation and incorporation into virions at the nonpermissive temperature. Virology 326, 288–298.

Sjaak de Wit, J.J., Cook, J.K., van der Heijden, H.M., 2011. Infectious bronchitis virus variants: a review of the history, current situation and control measures. Avian Pathol. 40, 223–235.

Tay, F.P., Huang, M., Wang, L., Yamada, Y., Liu, D.X., 2012. Characterization of cellular furin content as a potential factor determining the susceptibility of cultured human and animal cells to coronavirus infectious bronchitis virus infection. Virology 433, 421–430.

Thackray, L.B., Holmes, K.V., 2004. Amino acid substitutions and an insertion in the spike glycoprotein extend the host range of the murine coronavirus MHV-A59. Virology 324, 510–524.

Tsai, J.C., Zelus, B.D., Holmes, K.V., Weiss, S.R., 2003. The N-terminal domain of the murine coronavirus spike glycoprotein determines the CEACAM1 receptor specificity of the virus strain. J. Virol. 77, 841–850.
Wickramasinghe, I.N., de Vries, R.P., Grone, A., de Haan, C.A., Verheije, M.H., 2011. Binding of avian coronavirus spike proteins to host factors reflects virus tropism and pathogenicity. J. Virol. 85, 8903–8912.
Winter, C., Herrler, G., Neumann, U., 2008. Infection of the tracheal epithelium by infectious bronchitis virus is sialic acid dependent. Microbes Infect. 10, 367–373.
Winter, C., Schwegmann-Wessels, C., Cavanagh, D., Neumann, U., Herrler, G., 2006. Sialic acid is a receptor determinant for infection of cells by avian Infectious bronchitis virus. J. Gen. Virol. 87, 1209–1216.
Yamada, Y., Liu, D.X., 2009. Proteolytic activation of the spike protein at a novel RRRR/S motif is implicated in furin-dependent entry, syncytium formation, and infectivity of coronavirus infectious bronchitis virus in cultured cells. J. Virol. 83, 8744–8758.
Yamada, Y., Liu, X.B., Fang, S.G., Tay, F.P., Liu, D.X., 2009. Acquisition of cell–cell fusion activity by amino acid substitutions in spike protein determines the infectivity of a coronavirus in cultured cells. PLoS One 4, e6130.
Zhang, Y., Buckles, E., Whittaker, G.R., 2012. Expression of the C-type lectins DC-SIGN or L-SIGN alters host cell susceptibility for the avian coronavirus, infectious bronchitis virus. Vet. Microbiol. 157, 285–293.
Zheng, Q., Deng, Y., Liu, J., van der Hoek, L., Berkhout, B., Lu, M., 2006. Core structure of S2 from the human coronavirus NL63 spike glycoprotein. Biochemistry 45, 15205–15215.
Zhong, Y., Tan, Y.W., Liu, D.X., 2012. Recent progress in studies of arterivirus- and coronavirus–host interactions. Viruses 4, 980–1010.